

Emission characteristics of optically pumped GaN-based vertical-cavity surface-emitting lasers

Jung-Tang Chu, Tien-Chang Lu, Min You, Bor-Jye Su, Chih-Chiang Kao, Hao-Chung Kuo, and Shing-Chung Wang

Citation: *Applied Physics Letters* **89**, 121112 (2006); doi: 10.1063/1.2355476

View online: <http://dx.doi.org/10.1063/1.2355476>

View Table of Contents: <http://scitation.aip.org/content/aip/journal/apl/89/12?ver=pdfcov>

Published by the [AIP Publishing](#)

Articles you may be interested in

[Blue 6-ps short-pulse generation in gain-switched InGaN vertical-cavity surface-emitting lasers via impulsive optical pumping](#)

Appl. Phys. Lett. **101**, 191108 (2012); 10.1063/1.4766290

[Continuous wave operation of current injected GaN vertical cavity surface emitting lasers at room temperature](#)

Appl. Phys. Lett. **97**, 071114 (2010); 10.1063/1.3483133

[Fabrication and performance of blue GaN-based vertical-cavity surface emitting laser employing AlN GaN and Ta₂O₅ SiO₂ distributed Bragg reflector](#)

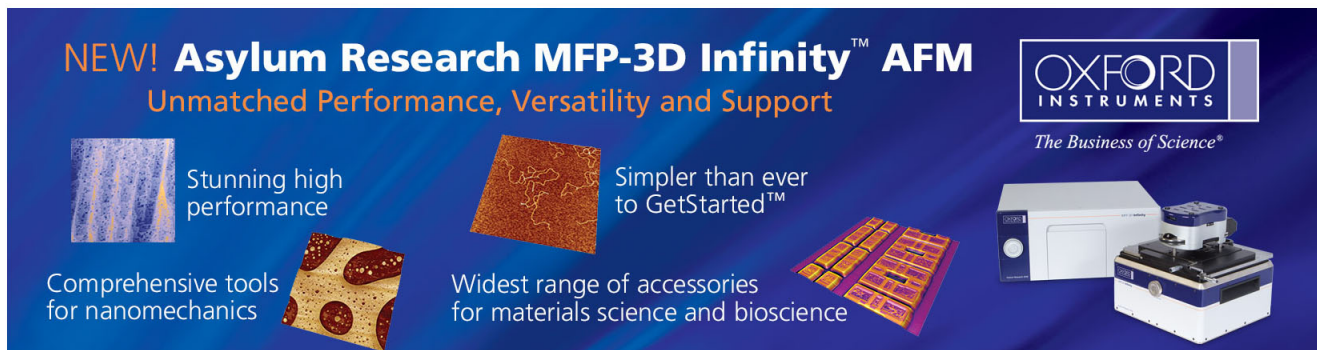
Appl. Phys. Lett. **87**, 081105 (2005); 10.1063/1.2032598

[Low-threshold lasing of InGaN vertical-cavity surface-emitting lasers with dielectric distributed Bragg reflectors](#)

Appl. Phys. Lett. **83**, 830 (2003); 10.1063/1.1596728

[Observation of enhanced spontaneous emission coupling factor in nitride-based vertical-cavity surface-emitting laser](#)

Appl. Phys. Lett. **80**, 722 (2002); 10.1063/1.1430855

The advertisement features a dark blue background with white and orange text. At the top left, it reads 'NEW! Asylum Research MFP-3D Infinity™ AFM' in large white letters, followed by 'Unmatched Performance, Versatility and Support' in orange. On the right, the Oxford Instruments logo is shown with the tagline 'The Business of Science®'. Below the text are four images: a textured surface, a circular pattern, a grid of small squares, and the physical AFM instrument. Text boxes describe the performance, ease of use, and accessory range of the instrument.

NEW! Asylum Research MFP-3D Infinity™ AFM
Unmatched Performance, Versatility and Support

OXFORD INSTRUMENTS
The Business of Science®

Stunning high performance

Simpler than ever to GetStarted™

Comprehensive tools for nanomechanics

Widest range of accessories for materials science and bioscience

Emission characteristics of optically pumped GaN-based vertical-cavity surface-emitting lasers

Jung-Tang Chu, Tien-Chang Lu, Min You, Bor-Jye Su, Chih-Chiang Kao, Hao-Chung Kuo, and Shing-Chung Wang^{a)}
 Department of Photonics, National Chiao Tung University, 1001 Ta Hsueh Road, Hsinchu, Taiwan 300,
 Taiwan and Institute of Electro-Optical Engineering, National Chiao Tung University, 1001 Ta
 Hsueh Road, Hsinchu, Taiwan 300, Taiwan

(Received 5 July 2006; accepted 5 August 2006; published online 20 September 2006)

The laser emission characteristics of a GaN-based vertical-cavity surface-emitting laser with two dielectric distributed Bragg reflectors were investigated under optically pumped operation at room temperature. The laser emitted wavelength at 415.9 nm with an emission linewidth of 0.25 nm and threshold pumping energy of 270 nJ. The laser has a high characteristic temperature of about 278 K and high spontaneous emission coupling factor of 10^{-2} . The laser emission showed single and multiple spot emission patterns with spectral and spatial variations under different pumping conditions. © 2006 American Institute of Physics. [DOI: 10.1063/1.2355476]

GaN-based blue/violet vertical-cavity surface-emitting lasers (VCSELs) have attracted much attention due to many advantageous properties over edge-emitting lasers, including circular beam shapes, light emission in the vertical direction, and two-dimensional arrays on the wafer level. A VCSEL structure is made up by a microcavity with a few wavelengths in length and a pair of high reflectivity (above 99%) distributed Bragg reflectors (DBRs) necessary for reducing the lasing threshold. Efforts to obtain optically pumped stimulated emission in GaN-based VCSELs have been reported by several groups.¹⁻⁴ Somlya *et al.*¹ and Zhou *et al.*² demonstrated lasing operations of VCSELs with the structure of monolithically grown AlGaIn/GaN DBRs, GaN/InGaIn microcavities, and dielectric DBRs.² GaN-based VCSELs with two dielectric DBRs were also proposed by Song *et al.*³ and Tawara *et al.*⁴ Our group has demonstrated initial lasing behaviors in two types of GaN VCSELs: one with hybrid-type DBRs which has a dielectric DBR and an epitaxially grown AlN/GaN DBR,⁵ the other is a dielectric-type VCSEL comprising a GaN active region and two dielectric DBRs.⁶ In this study, we report the detailed laser emission properties of the dielectric-type GaN-based VCSEL optically pumped at room temperature. The below and above threshold behaviors of laser emission intensity and temperature dependence of the threshold pumping energy were investigated. High spontaneous emission factor and high characteristic temperature were obtained. The laser emission properties showed the dependence of emission spectrum on pumping energy. Single and multiple spot emission patterns were observed spatially and spectrally, indicating a highly inhomogeneous gain distribution in the InGaIn/MQW layers.

The VCSEL layer structure grown on a (0001)-oriented sapphire substrate by metal organic chemical vapor deposition included a 30 nm GaN nucleation layer, a 4 μm GaN bulk layer, MQWs consisting of ten periods of 5 nm GaN barriers and 3 nm $\text{In}_{0.1}\text{Ga}_{0.9}\text{N}$ wells, and a 200 nm GaN cap layer. Six pairs of SiO_2 and TiO_2 were evaporated on the top of the grown VCSEL structure to form the first dielectric DBR. The reflectivity of the $\text{SiO}_2/\text{TiO}_2$ DBR at 416 nm was

99.5%. Next, an array of circular $\text{SiO}_2/\text{TiO}_2$ DBR mesas with diameters of 60 μm was formed by standard lithography and chemical wet etching process. To deposit the second dielectric DBR, the structure was subjected to a laser lift-off (LLO) process using a KrF excimer laser to remove the sapphire substrate. The GaN surface after LLO was further polished and obtained a surface roughness of about 1 nm for deposition of the second dielectric DBR consisting of eight pairs of SiO_2 and Ta_2O_5 . The final thickness of the epitaxial structure after LLO and polishing process was about 4 μm . The Ta_2O_5 was used to reduce the absorption of the pumping beam at a wavelength of 355 nm. The reflectivity of the $\text{SiO}_2/\text{Ta}_2\text{O}_5$ DBR at 416 nm was 97%. For the detailed process procedure, please refer to our previous report.⁶

Figure 1(a) shows the microscopic image of a fabricated

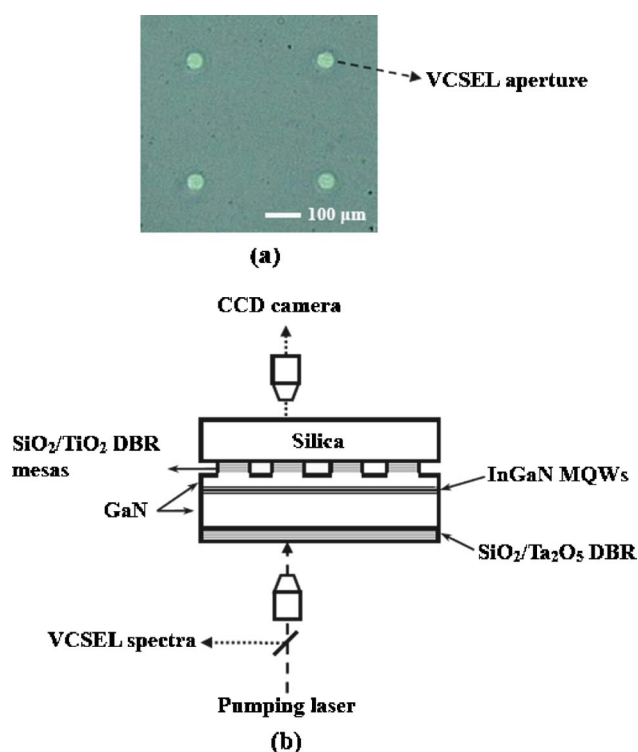


FIG. 1. (Color online) (a) Microscopic top view image of a 2×2 VCSEL array. (b) Schematic structure of the VCSEL and experiment setup.

^{a)}Electronic mail: sewang@cc.nctu.edu.tw

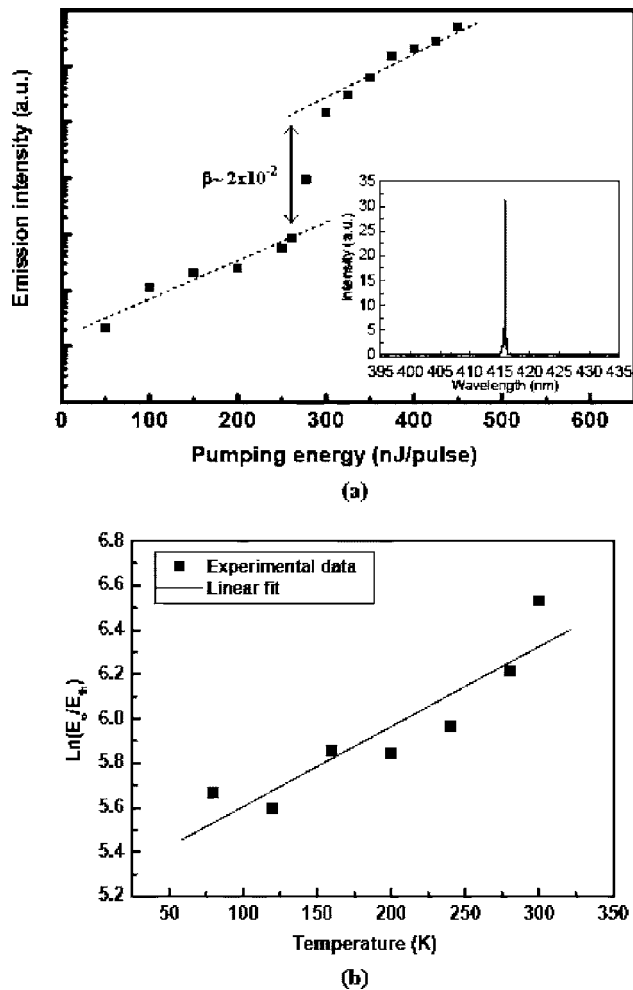


FIG. 2. (a) Laser emission intensity vs pumping energy in semilogarithmic scale. The β value estimated from the difference between the two dashed lines is about 2×10^{-2} . The inset shows the spectrum of the laser emission with a wavelength of 415.9 nm and a linewidth of about 0.25 nm. (b) Temperature dependence of the lasing threshold pumping energy (E_{th}) and the estimated T_0 of 278 K.

2×2 VCSEL array. The circular areas are the locations of VCSELs with DBRs, also serving the emission apertures. The fabricated GaN-based VCSELs were optically pumped by a Nd:YVO₄ laser at 355 nm, with a repetition rate of 1 kHz and a pulse width of 0.5 ns. As shown in Fig. 1(b), the pumping laser beam with a focused spot size of about 40 μm in diameter was vertically incident on the VCSEL sample from the SiO₂/Ta₂O₅ DBR side. The light emission from the VCSEL sample was collected by an imaging optic into a spectrometer with a spectral resolution of 0.1 nm. The emission patterns were detected by a charge coupled device camera from the SiO₂/TiO₅ DBR side through the mesa aperture. The dependence of threshold pumping energies on the temperature was measured from 58 to 322 K using a temperature-controlled cryogenic chamber.

The laser emission intensity as the function of pumping energy is shown in Fig. 2(a) in a semilogarithmic scale. A clear evidence of threshold behavior was observed at a pumping energy of $E_{th}=270$ nJ corresponding to an energy density of 21.5 mJ/cm². The inset shows the spectrum of the laser emission with a wavelength of 415.9 nm and a narrow linewidth of about 0.25 nm. From the semilogarithmic data, the spontaneous emission factor β , which indicated the coupling efficiency of the spontaneous emission to the lasing

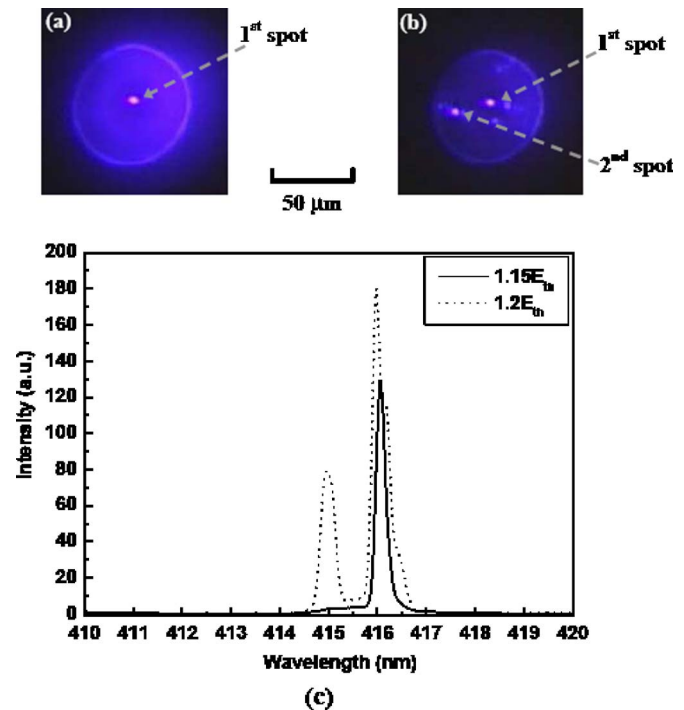


FIG. 3. (Color online) Emission pattern of the VCSEL at pumping energies of (a) $1.15E_{th}$ with single laser emission spot and (b) $1.2E_{th}$ with two laser emission spots. The arrows indicate the position of the first and second emission spots. (c) Spectra of the first emission spot and second emission spot at pumping energies of $1.15E_{th}$ and $1.2E_{th}$, respectively.

mode, was estimated from the difference between the heights of the emission intensities before and after lasing was estimated as about 2×10^{-2} , which was in agreement with the reported results^{4,7} and was nearly three orders of magnitude higher than that of the typical GaN edge-emitting semiconductor lasers,¹ indicating the enhancement of the spontaneous emission into a lasing mode by the high cavity quality factor (cavity Q factor) of the microcavity of the VCSEL structure.

The temperature dependence of the lasing threshold of the VCSEL is shown in Fig. 2(b). The threshold pumping energy increased gradually with increasing temperature. The dependence of the threshold condition on the temperature can be expressed as $E_{th}(T)=E_0 \exp(T/T_0)$, where E_0 is a constant and T_0 is the characteristic temperature. We obtain a characteristic temperature of about 278 K for this dielectric-type VCSEL for the temperature range of 58–322 K by linearly fitting the experimental result. This T_0 value is close to the T_0 value of 300 K for GaN-based VCSELs predicted by Honda *et al.*,⁸ and higher than the reported T_0 of 170 K (Ref. 9) or 235 K (Ref. 10) for the GaN-based edge-emitting laser diode. This T_0 value is also higher than the T_0 value for the hybrid DBR VCSEL we reported earlier.¹¹ The high T_0 value could be attributed to a better gain alignment of the MQWs with the cavity mode and a lower threshold carrier density due to the higher quality factor provided by both dielectric DBRs.

The laser emission patterns from the aperture show single spot and multiple spot emission patterns under different pumping conditions, as shown in Figs. 3(a) and 3(b) at pumping energies of $1.15E_{th}$ and $1.2E_{th}$. The lasing wavelength from each emission spot also differed in few nanometers. At low pumping energy, the emission pattern showed a single spot with a spot size of about 3 μm . As the pumping

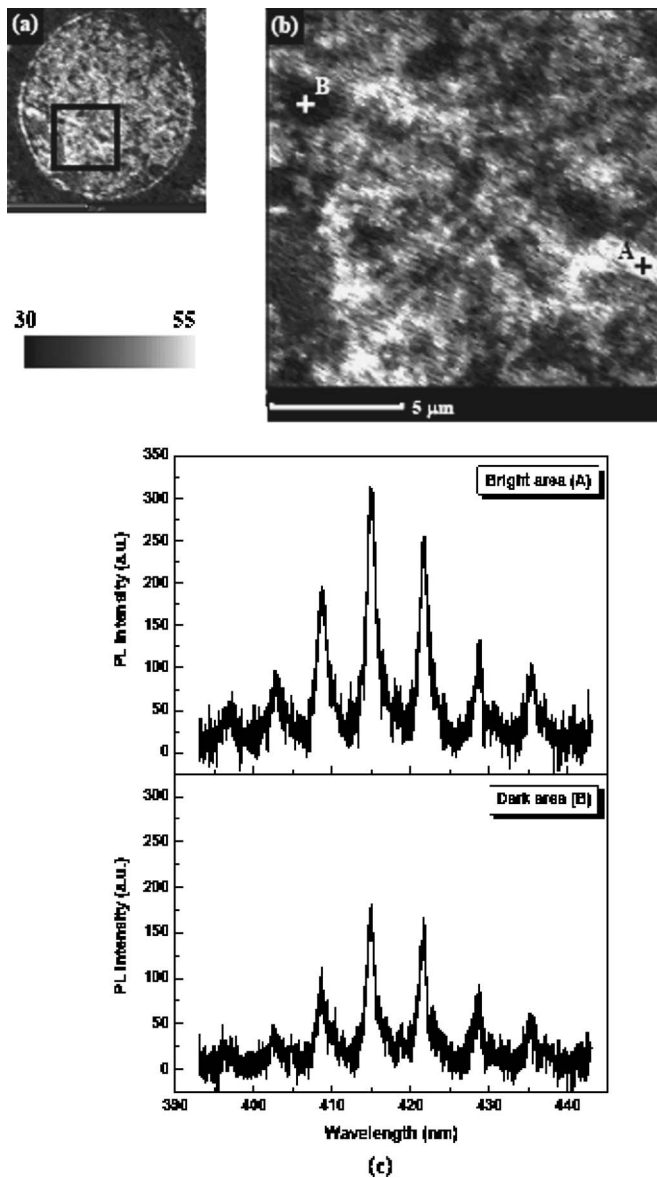


FIG. 4. (a) Micro-PL intensity mapping image of the VCSEL aperture. (b) Fine micro-PL scan inside the square area in (a). (c) PL spectra of bright (point A) and dark (point B) areas.

energy increased, a second spot appeared showing a double spot emission pattern with a spatial separation of about $22 \mu\text{m}$ apart. The corresponding emission spectra of these two spots are shown in Fig. 3(c). The wavelength of the single emission spot is about 415.9 nm. For the double emission pattern, there is second emission wavelength at about 414.9 nm in addition to the 415.9 nm emission line. Since the separation between these two spots is large compared to the axial mode spacing, the difference of the emission wavelengths could be caused by either the spatial nonuniformity in InGaN MQWs or the nonuniformity in the DBR cavity. To clarify the origin of these emission wavelength variations through the aperture, we conducted the microphotoluminescence (PL) intensity mapping of the VCSEL using a scanning optical microscopy. Figure 4(a) shows the intensity mapping of the entire aperture of the VCSEL. With a fine scan inside the square area in Fig. 4(a), Fig. 4(b) shows that the nonuniform PL emission intensity across the aperture has patches of bright areas with about $2\text{--}4 \mu\text{m}$ in size. The bright areas have about 1.8 times higher intensity than the

dark areas. Figure 4(c) shows the PL spectra of bright (marked as A) and dark (marked as B) areas. Nevertheless, spatial inhomogeneity in cavity loss due to potential micrometer-scale imperfection of the DBRs could also cause different threshold gains in spatial distribution. However, micro-PL measurement results in Fig. 4(c) show a similar linewidth of the spontaneous emission for bright and dark areas, indicating no significant spatially nonuniformity in the DBRs across the circular mesa. On the other hand, the different micro-PL intensities across the VCSEL aperture imply a nonuniform material gain distribution existed in InGaN/GaN MQW layers. In fact, the indium fluctuation was commonly observed for the epitaxially grown InGaN MQWs and also the subsequent carrier localization effect had been reported.¹² Therefore, we believe that the indium inhomogeneity in the VCSEL MQWs could be responsible for the appearance of spatially separated lasing spots within the mesa aperture, and the difference in the emission wavelength could be due to the slight variation in the indium content of the MQW.

In summary, the laser emission characteristics of a GaN-based VCSEL with two dielectric DBRs were investigated under optical pumping at room temperature. The laser emits an emission wavelength at 415.9 nm with a linewidth of 0.25 nm. The laser has a threshold pumping energy of 270 nJ at room temperature and a characteristic temperature of 278 K. The VCSEL has a high spontaneous emission factor of about 2×10^{-2} . The laser emission patterns show single and multiple emission spots spatially with different emission spectra under different pumping conditions. The inhomogeneous material gain distribution could be due to the fluctuated indium composition in the MQW active layers and could lead to remarkable spatial and spectral broadenings in laser emission properties and degrade the VCSEL performance.

This work was supported by the MOE ATU program and in part by the National Science Council of Republic of China (ROC) in Taiwan under Contract Nos. NSC 93-2120-M-009-006, NSC 93-2752-E-009-008-PAE, and NSC 93-2215-E-009-068.

¹T. Someya, R. Werner, A. Forchel, M. Catalano, R. Cingolani, and Y. Arakawa, *Science* **285**, 1905 (1999).

²H. Zhou, M. Diagne, E. Makarona, A. V. Nurmikko, J. Han, K. E. Waldrip, and J. J. Figiel, *Electron. Lett.* **36**, 1777 (2000).

³Y. K. Song, H. Zhou, M. Diagne, A. V. Nurmikko, R. P. Schneider, Jr., C. P. Cuo, M. R. Krames, R. S. Kern, C. Carter-Coman, and F. A. Kish, *Appl. Phys. Lett.* **76**, 1662 (2000).

⁴T. Tawara, H. Gotoh, T. Akasaka, N. Kobayashi, and T. Saitoh, *Appl. Phys. Lett.* **83**, 830 (2003).

⁵C. C. Kao, Y. C. Peng, H. H. Yao, J. Y. Tsai, Y. H. Chang, J. T. Chu, H. W. Huang, T. T. Kao, T. C. Lu, H. C. Kuo, and S. C. Wang, *Appl. Phys. Lett.* **87**, 081105 (2005).

⁶J. T. Chu, T. C. Lu, H. H. Yao, C. C. Kao, W. D. Liang, J. Y. Tsai, H. C. Kuo, and S. C. Wang, *Jpn. J. Appl. Phys., Part 1* **45**, 2556 (2006).

⁷S. Kako, T. Someya, and Y. Arakawa, *Appl. Phys. Lett.* **80**, 722 (2002).

⁸T. Honda, H. Kawanishi, T. Sakaguchi, F. Koyama, and K. Iga, *MRS Internet J. Nitride Semicond. Res.* **4S1**, G6.2 (1999).

⁹C. Skierbiszewski, P. Perlin, I. Grzegory, Z. R. Wasilewski, M. Siewacz, A. Feduniewicz, P. Wisniewski, J. Borysiuk, P. Prystawko, G. Kamler, T. Suski, and S. Porowski, *Semicond. Sci. Technol.* **20**, 809 (2005).

¹⁰M. Ikeda and S. Uchida, *Phys. Status Solidi A* **194**, 407 (2002).

¹¹Chih-Chiang Kao, T. C. Lu, H. W. Huang, J. T. Chu, Y. C. Peng, H. H. Yao, J. Y. Tsai, T. T. Kao, H. C. Kuo, S. C. Wang, and C. F. Lin, *IEEE Photonics Technol. Lett.* **18**, 877 (2006).

¹²K. Okamoto, A. Kaneta, Y. Kawakami, S. Fujita, J. Choi, M. Terazima, and T. Mukai, *J. Appl. Phys.* **98**, 064503 (2005).